BIOCHEMISTRY
including biophysical chemistry & molecular biology

Article

pubs.acs.org/biochemistry

Differential Effects of Familial Parkinson Mutations in LRRK2 Revealed by a Systematic Analysis of Autophosphorylation

Shogo Kamikawaji,[†,§] Genta Ito,[‡,§] Tomoko Sano,[†] and Takeshi Iwatsubo*[,†,‡]

[†]Department of Neuropathology and Neuroscience, Graduate School of Pharmaceutical Sciences, The University of Tokyo, 7-3-1 Hongo, Bunkyoku, Tokyo, 113-0033 Japan

[‡]Department of Medicine, Graduate School of Neuropathology, The University of Tokyo, 7-3-1 Hongo, Bunkyoku, Tokyo, 113-0033 Japan

Supporting Information

ABSTRACT: Mutations in the *leucine-rich repeat kinase 2* (*LRRK2*) gene have been identified in pedigrees of autosomal-dominant familial Parkinson's disease (PARK8). It has been shown that the kinase activity of LRRK2 is required for its neuronal toxicity, although how familial Parkinson mutations affect the function of LRRK2 has not been well characterized. In the present study, we systematically characterized the autophosphorylation of LRRK2 by phosphopeptide mapping and identified Thr1348, Thr1349, and Thr1357 as the major autophosphorylation sites. We found that the autophosphorylation at Thr1357 is downregulated by the Y1699C mutation, possibly through a conformational alteration of the ROC domain. We also found that I2020T mutant LRRK2 undergoes excessive autophosphorylation in cell lysates in vitro at a low concentration of ATP. These results highlight the differential effects of familial mutations in LRRK2 on its conformation and enzymatic properties.

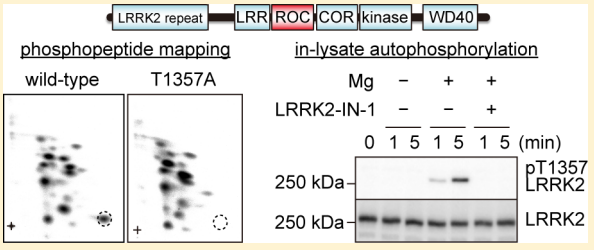

Parkinson's disease (PD) is one of the most common neurodegenerative disorders in adulthood and is pathologically characterized by nigral degeneration accompanied by Lewy body formation.[1−3] The *LRRK2* gene has been identified as the causative gene for PARK8, an autosomal-dominant inherited form of familial PD (FPD).[4,5] Patients harboring LRRK2 mutations develop PD with typical clinical manifestations,[6] implicating a common mechanism underlying the pathogenesis of PARK8 and sporadic PD. In fact, two independent genome-wide association studies have recently identified single-nucleotide polymorphisms around the LRRK2 locus as a common risk for sporadic PD.[7,8]

LRRK2 codes for a large multidomain protein containing two distinct enzymatic domains: a ROC (Ras of complex proteins) domain and a protein kinase domain, the former being responsible for GTP binding, which is required for the kinase activity[9−12] (Figure 1A). In addition, LRRK2 has a domain with unknown function named the COR (carboxyl-terminal of ROC) domain, which is located between the two functional domains. Six missense mutations (R1441C/G/H, Y1699C, G2019S, and I2020T) linked to PARK8 have been reported within these three functional domains[13] (Figure 1A), suggesting that abnormality in the structure and functions of these domains plays a critical role in the pathogenesis of PARK8. The kinase activity of LRRK2 has been implicated in the neuronal toxicity caused by overexpression of familial mutant forms of LRRK2 because the introduction of mutations inactivating the LRRK2 kinase activity mitigated the toxicity.[10] It has repeatedly been shown that the G2019S mutation, which is the most frequently identified, especially in Ashkenazi Jews,[14] increases the kinase activity of LRRK2 in vitro.[15] These results suggest that upregulation of the kinase activity is the key pathogenic phenotype of LRRK2 mutations linked to PD. However, the abnormal increase in the kinase activity of LRRK2 has not been reproducibly demonstrated in mutations other than G2019S.[16−19] Thus, it is still unclear whether the pathogenic effects caused by all of the PD mutations of LRRK2 are common or, alternatively, whether each mutation has different effects.

The ezrin/radixin/moesin (ERM) family proteins, microtubule-associated protein Tau, and Endophilin A have been characterized as in vitro substrates of LRRK2.[17,20,21] However, the specificity and the physiological relevance of the phosphorylation of these proteins by LRRK2 has not been established. Besides phosphorylating substrates, protein kinases, including LRRK2, often phosphorylate themselves (i.e., autophosphorylation), which is often used as a surrogate for evaluating the kinase activity.[22] Although a set of autophosphorylation sites of LRRK2 have been identified through one-by-one analyses by mass spectrometry,[23−27] the complete picture of autophosphorylation has not been described. Moreover, the lack of quantitativity in mass spectrometry makes it difficult to identify the major autophosphorylation sites with a higher extent of phosphorylation.

Received: May 12, 2013
Revised: July 19, 2013
Published: August 8, 2013

   dx.doi.org/10.1021/bi400596m | *Biochemistry* 2013, 52, 6052−6062

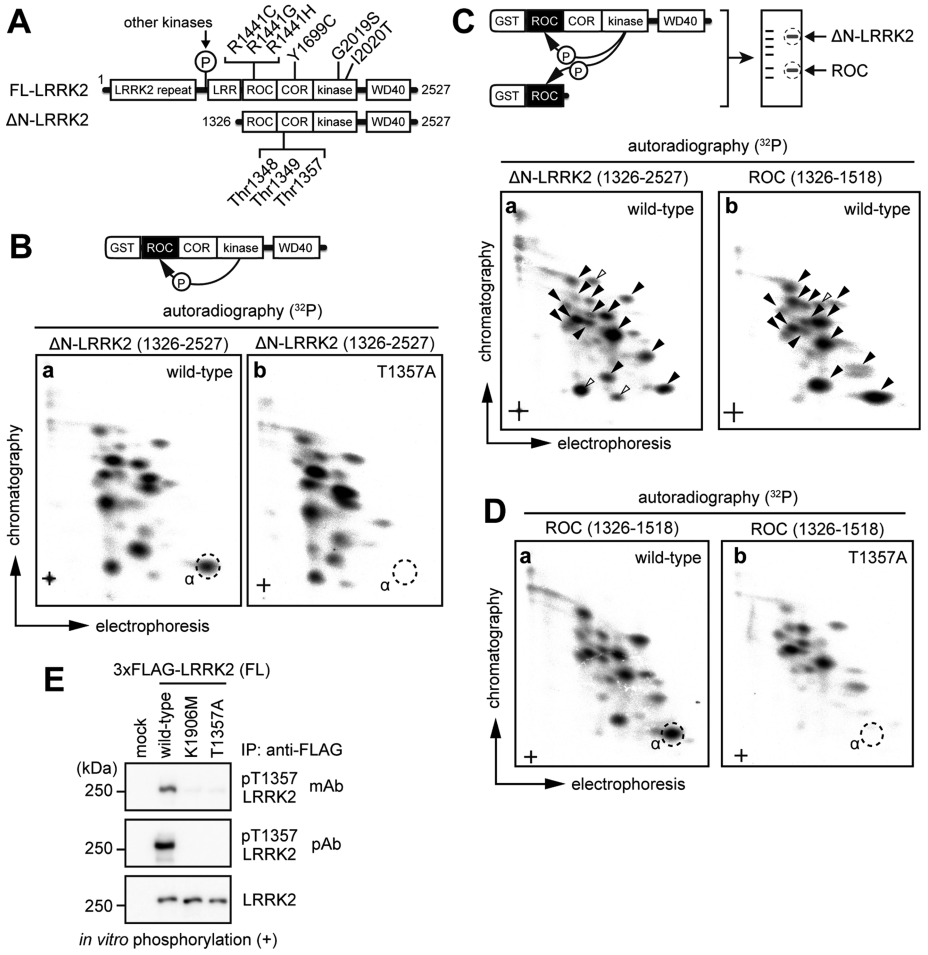

Figure 1. Identification of major autophosphorylation sites of LRRK2 by 2D thin-layer chromatography (2D TLC) analysis. (A) Schematic representation of full-length (FL) LRRK2 and ΔN-LRRK2 (1326−2527 aa). The familial mutations as well as the autophosphorylated residues identified in this study are shown. (B) 2D TLC map of GST-ΔN-LRRK2. WT (a) and T1357A (b) GST-ΔN-LRRK2 were purified, autophosphorylated in vitro in the presence of [γ-^{32}P] ATP, and subjected to 2D TLC analysis. The spot α surrounded by dotted lines disappeared in the map of T1357A ΔN-LRRK2. The plus sign (+) on the map indicates the position where the sample was applied. (C) Comparison of the 2D TLC maps between GST-ΔN-LRRK2 and GST-ROC. Sf9 cells were infected with baculovirus harboring cDNA encoding GST-ΔN-LRRK2 or the ROC domain (1326−1518 aa). Overexpressed GST-fusion polypeptides were affinity-purified using glutathione Sepharose. Purified ΔN-LRRK2 was autophosphorylated in vitro in the presence of [γ-^{32}P] ATP (a), whereas purified GST-ROC was incubated with GST-ΔN-LRRK2 in the presence of [γ-^{32}P] ATP to be phosphorylated in trans (b). The radioactive bands corresponding to GST-ΔN-LRRK2 and GST-ROC were cut out from the blotted membrane and subjected to 2D TLC analysis. Spots observed in both ΔN-LRRK2 and ROC are marked with black arrowheads, and those observed in either blot are marked with white arrowheads. (D) 2D TLC map of GST-ROC. GST-ROC (WT or T1357A) or GST-ΔN-LRRK2 (WT) was transfected into HEK293 cells, affinity-purified, and subjected to in-trans autophosphorylation in the presence of [γ-^{32}P] ATP. After separation by SDS-PAGE, the band corresponding to GST-ROC was subjected to 2D TLC analysis. The spot α surrounded by dotted lines disappeared in the map of GST-ROC harboring the T1357A mutation. (E) Autophosphorylation at Thr1357 in FL-LRRK2. Immunoprecipitated and in vitro phosphorylated FL-LRRK2 was subjected to immunoblotting with the rat monoclonal (mAb; top panel) and the rabbit polyclonal (pAb; middle panel) anti-pT1357 antibodies. Total LRRK2 was detected by immunoblotting with the anti-LRRK2 antibody (MJFF2; bottom panel).

In this study, we adopted the phosphopeptide mapping method for the systematic characterization of the autophosphorylation of LRRK2 and identified Thr1348, Thr1349, and Thr1357 within the ROC domain as the major autophosphorylation sites in vitro. In addition, we established a unique in-lysate kinase assay system using the autophosphorylation at Thr1357 as a sensitive marker for the kinase activity of LRRK2. We further characterized the different effects of familial PD mutations on the kinase properties of LRRK2.

EXPERIMENTAL PROCEDURES

Construction of Expression Plasmids. For mammalian expression, full-length (FL) human LRRK2 cloned in the p3×FLAG-CMV-10 vector (Sigma) and ΔN-LRRK2 (1326−2527 aa) cloned in the pDEST27 vector (Life Technologies) were constructed as described previously.[11,24] The bacterial expression vector encoding GST-LRRKtide was generated as described previously.[24] For the baculovirus/Sf9 expression system, ΔN-LRRK2 and ROC (1326−1518 aa) fragments cloned in the pENTR/TEV/D-TOPO vector (Life Technologies) were cut and ligated into the pDEST20 vector (Life Technologies). Nucleotide substitution was introduced into a fragment less than 1.5 kb in size by a long PCR protocol. The sequences of the PCR primers used are listed in the Supporting Information. Mutated fragments were subsequently ligated into FL-LRRK2 or ΔN-LRRK2 by appropriate digestion and ligation. All constructs generated from PCR products were verified by DNA sequencing.

dx.doi.org/10.1021/bi400596m | Biochemistry 2013, 52, 6052−6062

Cell Culture and Transfection. Human embryonic kidney (HEK) 293 cells and human lung carcinoma A549 cells were maintained in Dulbecco's modified Eagle's medium (DMEM) supplemented with 10% (v/v) fetal bovine serum, 100 units/ml of penicillin, and 100 μg/mL of streptomycin at 37 °C in a 5% CO_2 atmosphere. Transient expression in HEK293 cells was performed by transfecting the plasmids using FuGENE6 (Roche) or polyethyleneimine (Sigma) according to the manufacturer's protocol. When indicated, the cells were treated with LRRK2-IN-1 (provided by Dr. Dario Alessi, University of Dundee) dissolved in DMSO. Sf9 cells were cultured in Grace's supplemented media (Life Technologies) containing 10% (v/v) fetal bovine serum, 0.1% (v/v) Pluronic F-68 (Life Technologies), 100 units/ml of penicillin, and 100 μg/mL of streptomycin (Life Technologies) in a 1 L spinner flask at 27 °C. Protein expression in Sf9 cells and the purification of the GST-fusion proteins were conducted as described previously.[24]

Generation of the Anti-pT1357 Antibodies. The rabbit polyclonal anti-pT1357 antibody was raised against an amino-terminally KLH (keyhole limpet hemocyanin)-conjugated synthetic phosphopeptide KLH-Cys-QLMKpTKKSD (BEX), where pT stands for phosphorylated Thr. The antisera were affinity purified using SulfoLink Resin columns (ThermoFisher Scientific) conjugated with the phosphopeptide. Phosphorylation-independent antibodies were eliminated by passing through a column conjugated with a nonphosphorylated immunogen peptide, and the flow-through fractions were collected and used for the experiments. The rat monoclonal anti-pT1357 antibody was raised against a phosphopeptide, KLH-Cys-QLMKpTKKSD-amide (BEX). The inguinal and celiac lymph nodes of the immunized rats were collected, and the extracted B cells were fused with mouse myeloma PEI cells by the poly(ethylene glycol) method.[3,28] Hybridoma selection was carried out in GIT media (WAKO) supplemented with HAT or HT (Sigma), 10% (v/v) BM condimed H1 (Roche), 100 units/ml of penicillin, 100 μg/mL of streptomycin, 0.29 mg/mL of L-Glutamine, and 10% (v/v) fetal bovine serum. After obtaining monoclonal hybridomas, the clone 52-1-3 was selected by screening the culture media of hybridomas containing secreted immunoglobulin with ELISA and immunoblotting. The culture media from clone 52-1-3 was collected and subjected to purification of the immunoglobulin using the HiTrap Protein G column (GE Healthcare) according to the manufacturer's instructions.

Antibodies and Immunochemical Analysis. The anti-pT1357 antibodies were generated as described above. The anti-pT1410 (#7125-1) and the anti-pT1491 (#7058-1) antibodies were from Epitomics. The anti-LRRK2 (NB300−268) was purchased from Novus Biologicals. The anti-LRRK2 (MJFF2; #3514-1) was from Epitomics. The anti-FLAG M2 antibody was from Sigma. Immunoprecipitation with the anti-FLAG antibody as well as immunoblotting was conducted as described previously.[29] For immunoblotting with phospho-specific antibodies, 3% BSA (bovine serum albumin; Sigma) solubilized in TBS-Tween (50 mM Tris-HCl (pH 7.6), 150 mM NaCl, and 0.1% (v/v) Tween-20) was used for blocking the membranes instead of 5% (w/v) skim milk/TBS-Tween.

Phosphopeptide Mapping by Two-Dimensional Thin-Layer Chromatography. Phosphopeptide mapping was performed as described previously with some modifications.[30] Proteins of interest were phosphorylated in the presence of [γ-^{32}P] ATP in an in vitro kinase reaction. The samples were then separated by SDS-PAGE and transferred onto a PVDF membrane (Millipore). The radioactive band corresponding to the protein of interest was dissected from the membrane and treated with 0.5% (w/v) poly(vinylpyrrolidone)-360 (Sigma) in 1% (v/v) acetic acid for 30 min at 37 °C. After sequential washes with distilled water and 50 mM NH_4HCO_3, the band was digested with TPCK-trypsin (Worthington) for 4 h at 37 °C. The supernatants were lyophilized, solubilized with the pH 1.9 solution (2.2% (v/v) formic acid and 7.8% (v/v) acetic acid (pH 1.9)), and spotted onto the cellulose plate (Merck). Equal radioactivity of samples was applied to the 2D TLC by measuring the radioactivity with a liquid scintillation counter. First dimension thin-layer electrophoresis was performed in the pH 1.9 solution using the NA-4000-B1000 V electrophoresis apparatus (Nihon Eido). After overnight drying, the plate was subjected to ascending chromatography by putting the plate into the developing chamber containing the phospho-chromatography solution (37.5% (v/v) *n*-butanol, 25% (v/v) pyridine, and 7.5% (v/v) acetic acid). Finally, the plate was air-dried and analyzed with the BAS-1800 image analyzer (FujiFilm).

Phosphorylation Analysis. The in vitro kinase assay using [γ-^{32}P] ATP as well as the metabolic labeling of cells with [^{32}P] orthophosphate was conducted as described previously.[11]

In Vitro Autophosphorylation in Cell Lysates. Transfected HEK293 cells or A549 cells in a 10 cm dish were lysed in 500 μL of the lysis buffer (50 mM Tris-HCl (pH 7.6), 150 mM NaCl, 0.5% NP-40, complete protease inhibitor cocktail (Roche), and PhosSTOP phosphatase inhibitor cocktail (Roche)). The protein concentration was determined using the BCA protein assay kit (Thermo) and adjusted to 0.5 mg/mL using the lysis buffer. Magnesium chloride was added to the lysate at a final concentration of 20 mM, and the lysate was incubated at 30 °C for the indicated periods. The reactions were stopped by the addition of 5× SDS-PAGE sample buffer (400 mM Tris-HCl (pH 6.8), 50% (v/v) glycerol, 10% (w/v) SDS, 5% (v/v) 2-mercaptoethanol, 0.0125% (w/v) brilliant green, and 0.03125% (w/v) CBB-G250), and the samples were subjected to SDS-PAGE and immunoblotting.

In Vitro Kinase Assay Using the anti-pT1357 Antibody. Assays were performed in 10 μL of the assay buffer (20 mM Tris-HCl (pH 7.5), 10 mM $MgCl_2$, 2 mM DTT, 0.02% (v/v) Tween-20, 520 μM bT1357tide (biotin-CQLMKTKKSD-amide; BEX), 30 ng GST-ΔN-LRRK2 (970−2527 aa; Life Technologies), protease inhibitor cocktail (complete EDTA-free; Roche), and phosphatase inhibitor cocktail (PhosSTOP; Roche)) and were initiated by adding ATP. After incubation for 15 to 60 min, the reactions were stopped by the addition of 190 μL of the stop solution (50 mM Tris-HCl (pH 7.6), 150 mM NaCl, 0.5% NP-40, and 20 mM EDTA). The bT1357tide was captured on the streptavidin-coated plate (ThermoFisher Scientific) by applying 50 μL of the reaction mixtures to the plate in triplicate. Phosphorylation of the captured bT1357tide was detected by ELISA using the anti-pT1357 antibody (rat monoclonal) as a primary antibody and an antirat IgG antibody conjugated with horseradish peroxidase (Jackson Immunoresearch) as a secondary antibody.

RESULTS

Phosphopeptide Mapping of Amino-Terminally Truncated LRRK2. Besides autophosphorylation, FL-LRRK2 (Figure 1A) is phosphorylated at multiple sites amino terminal to the LRR domain by other kinases in HEK293 cells,[31] which hampers the identification of autophosphorylation sites by mass spectrometry. In contrast, an amino-terminally truncated mutant

LRRK2 (ΔN-LRRK2; 1326−2527 aa; Figure 1A) is devoid of phosphorylation by other kinases because it lacks most of the major phosphorylation sites.[24] To systematically identify autophosphorylation sites of LRRK2, we conducted phosphopeptide mapping of ΔN-LRRK2 that was isolated from transfected HEK293 cells and phosphorylated in vitro in the presence of [γ-^{32}P] ATP. Phosphopeptide maps generated by separating the tryptic peptides of [^{32}P]-labeled ΔN-LRRK2 by 2D thin-layer chromatography (2D TLC) revealed a large number of spots corresponding to autophosphorylation (Figure 1B-a).

Identification of the Major Autophosphorylation Sites in the ROC Domain. Because the ROC domain was shown to be phosphorylated by LRRK2 in vitro,[23] we conducted phosphopeptide mapping of GST-ROC (1326−1518 aa) phosphorylated by GST-ΔN-LRRK2 (Figure 1C-b). The phosphopeptide map of GST-ROC exhibited a similar pattern to that of GST-ΔN-LRRK2 (black arrowheads in Figure 1C-a), suggesting that the majority of the spots observed in the map of ΔN-LRRK2 are attributable to the ROC domain. Because it has been reported that LRRK2 selectively phosphorylates Thr residues,[18,26] we next examined which Thr residue in the ROC domain is autophosphorylated by substituting all Thr residues in the ROC domain with Ala (T1343A, T1348A, T1349A, T1348A/T1349A, T1357A, S1366A/T1368A, T1404A, T1410A, T1452A, T1470A, T1491A, and T1503A/S1508A). An equal amount of radioactivity of the samples was applied to 2D TLC to exclude the variation in the kinase activity caused by the substitutions. When Thr1357 was substituted with Ala (T1357A) in GST-ΔN-LRRK2, the spot α disappeared (Figure 1B-b). In addition, the spot α also disappeared in the phosphopeptide map of GST-ROC harboring the T1357A substitution phosphorylated by GST-ΔN-LRRK2 (Figure 1D). These results suggested that the spot α corresponds to the peptides phosphorylated at Thr1357. Similarly, we found that substitutions at Thr1348 and Thr1349 altered the 2D TLC map (Figure S1A,1B). We generated rabbit polyclonal and rat monoclonal antibodies against a synthetic peptide containing phospho-Thr1357. Overexpressed and immunoprecipitated FL-LRRK2 was subjected to in vitro phosphorylation. Both antibodies reacted with wild-type (WT) LRRK2 but did not react with either the kinase-inactive K1906 M LRRK2 or T1357A LRRK2, which lacks the antigenic residue (Figure 1E). These results indicated that Thr1357 is autophosphorylated not only in ΔN-LRRK2 but also in FL-LRRK2.

Negative Regulation of the Kinase Activity by Autophosphorylation at Thr1349. The GTP-binding capacity of the ROC domain has been shown to be essential to the kinase activity because the nucleotide-free T1348N as well as K1347A LRRK2 lacks in vitro kinase activity.[11,32] Therefore, phosphorylation in the ROC domain might have a potential regulatory role not only in GTP binding but also in the kinase activity of LRRK2. To investigate the functional significance of the autophosphorylation identified in this study, we substituted Thr1348, Thr1349, and Thr1357 with Ala or Asp to mimic the constitutively dephosphorylated or phosphorylated states, respectively. Because we have confirmed that the autophosphorylation of these sites occurs in FL-LRRK2 (Figure 1E), we used FL-LRRK2 for the examination of their functional significance. We first investigated guanine-nucleotide (GTP and GDP) binding in cells by metabolic labeling and found that T1348A/D LRRK2 showed no detectable guanine-nucleotide binding (Figure 2A). This result is consistent with the fact that Thr1348 is essential to guanine-nucleotide binding.[11] Interestingly, T1349D LRRK2 bound no guanine nucleotides in cells, whereas T1349A LRRK2 bound a comparable amount of guanine nucleotides as that of WT LRRK2 (Figure 2A). This result suggested that autophosphorylation at Thr1349 has a functional role in guanine-nucleotide binding. Next, the kinase activity of these mutants was examined by autophosphorylation as well as by in vitro phosphorylation of

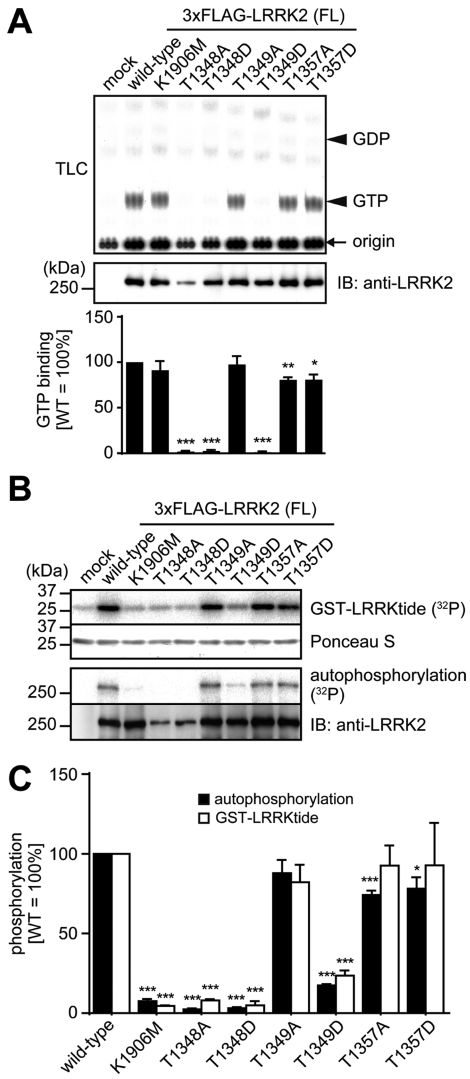

Figure 2. Functional role of the autophosphorylation in GTP binding and the kinase activity of LRRK2. (A) FL-3×FLAG-LRRK2 was immunoprecipitated from HEK293 cells metabolically labeled with [^{32}P]-orthophosphate, and the bound guanine nucleotides were analyzed by thin-layer chromatography (TLC). The levels of bound GTP were quantified and normalized to the expression levels of LRRK2. (B) FL-LRRK2 immunoprecipitated from transfected HEK293 cells was subjected to an in vitro kinase assay. The kinase activity for GST-LRRKtide (top panel) as well as the autophosphorylation activity (third panel from the top) was examined. The second panel from the top shows the Ponceau S staining of the membrane to show the equal level of loading of the GST-LRRKtide. (C) Quantification of panel B. The levels of the autophosphorylation (black) as well as the phosphorylation levels of GST-LRRKtide (white) were quantified and normalized to the expression levels of LRRK2 that were determined by immunoblotting with the anti-LRRK2 antibody (bottom panel in B). The data are given as the percentage of those observed in WT LRRK2 (n = 3, mean ± standard error). *p < 0.05, **p < 0.01, and ***p < 0.001 (Student's t test; compared with WT).

dx.doi.org/10.1021/bi400596m | Biochemistry 2013, 52, 6052−6062

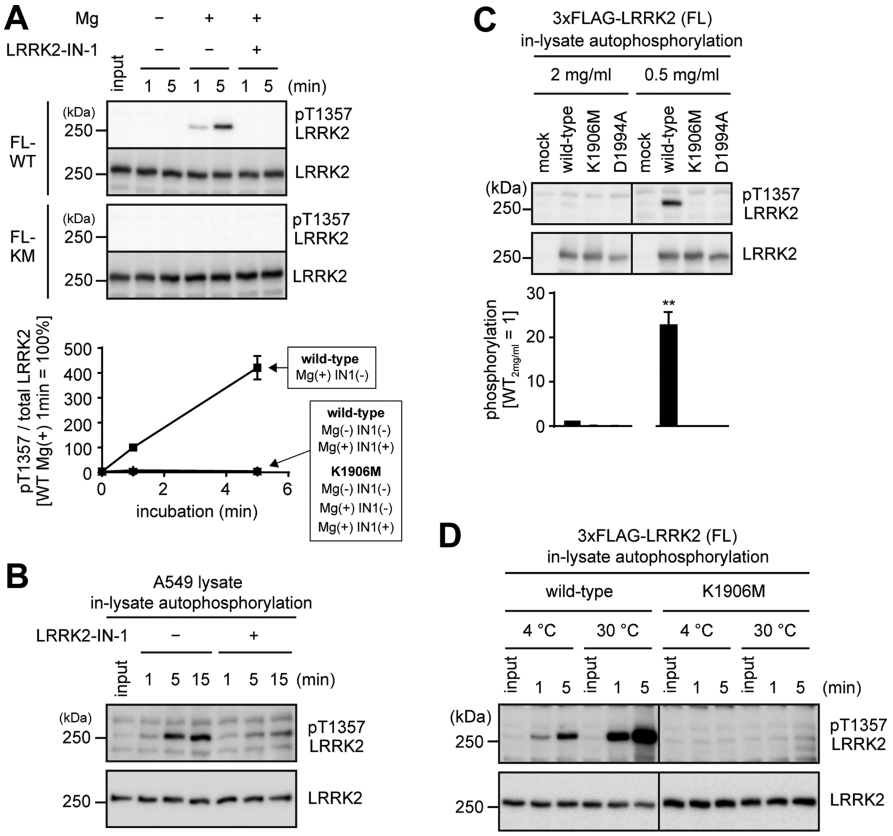

Figure 3. In-lysate autophosphorylation at Thr1357 of LRRK2. (A, B) HEK293 cells overexpressing FL-3×FLAG-LRRK2 (A) as well as A549 (B) cells were lysed in the buffer containing 0.5% NP-40. The lysates (0.5 mg/mL) were incubated at 30 °C for the indicated periods in the presence of 20 mM $MgCl_2$ and subjected to immunoblotting with the anti-pT1357 antibody (top panel). LRRK2-IN-1 dissolved in DMSO was added at a concentration of 3 μM. WT, wild type; KM, K1906M. (C) In-lysate autophosphorylation of LRRK2 at higher protein concentrations. The in-lysate autophosphorylation at Thr1357 was examined using two different protein concentrations of the cell lysates. The data are given as the ratio of those observed in 2 mg/mL lysates ($n = 3$, mean ± standard error). $^{**}p < 0.01$ (Student' t test; compared with WT LRRK2 in a 2 mg/mL lysate). (D) Temperature dependence of the in-lysate autophosphorylation of LRRK2. Lysates (0.5 mg/mL) of HEK293 cells overexpressing WT or K1906M LRRK2 were incubated in the presence of 20 mM $MgCl_2$ and 1 mM ATP for the indicated periods at 4 or 30 °C.

GST-LRRKtide.[18] As expected, T1348A LRRK2 and T1348D LRRK2 failed to exhibit kinase activity (Figure 2B,C). In addition, the T1349D substitution caused a significant reduction in the kinase activity, whereas the T1349A substitution had no effect (Figure 2B,C). These results suggested that autophosphorylation at Thr1349 has an inhibitory effect on the kinase activity by inhibiting guanine-nucleotide binding.

Autophosphorylation at Thr1357 in Cell Lysates. To examine whether LRRK2 is autophosphorylated at Thr1357 in cells, in vitro phosphorylation was omitted and cell lysates overexpressing FL-3×FLAG-LRRK2 were directly subjected to immunoblotting. Autophosphorylation at Thr1357 was not observed, indicating that autophosphorylation does not occur at this residue in cells (Figure 3A; input). Autophosphorylation at Thr1357 of FL-LRRK2 was not observed even after immunoprecipitation when in vitro phosphorylation was omitted (Figure S1C). Interestingly, when lysates of HEK293 cells overexpressing FL-LRRK2 were supplemented with 20 mM magnesium chloride and incubated at 30 °C for 5 min, a band labeled by the anti-pT1357 antibody was detected by immunoblotting (Figures 3A and S2A). The band disappeared by the addition of LRRK2-IN-1, a LRRK2-specific inhibitor (Figure 3A), and the band was not observed in K1906M LRRK2 (Figure 3A; FL-KM), ensuring that the band corresponds to the autophosphorylation of LRRK2 at Thr1357. We also showed that the endogenous level of expression of LRRK2 was sufficient for the detection of the in-lysate autophosphorylation at Thr1357 in human lung carcinoma-derived A549 cells (Figure 3B), in which we found a relatively high level of endogenous expression of LRRK2 (Figure S2B). In addition, we detected the in-lysate autophosphorylation not only at Thr1357 but also at Thr1410 and Thr1491 (Figure S2C). The in-lysate autophosphorylation at Thr1357 was diminished by prolonged incubation up to 24 h (Figure S2D), suggesting that phosphatases existing in cell lysates dephosphorylated the phosphorylation at Thr1357 after prolonged incubation. Less efficient autophosphorylation was observed in cell lysates with a higher protein concentration (Figure 3C), suggesting that unknown substances in cell lysates (e.g., phosphatase) inhibit autophosphorylation of LRRK2 in a concentration-dependent manner. Surprisingly, the in-lysate autophosphorylation at Thr1357 occurred at 4 °C, although the reaction took place less efficiently than that at 30 °C (Figure 3D). Collectively, these results suggested that LRRK2 efficiently undergoes autophosphorylation at Thr1357, although dephosphorylation dominates over the autophosphorylation in cell lysates after prolonged incubation or at higher protein concentration.

Effect of Guanine Nucleotide Analogs on In-Lysate Autophosphorylation at Thr1357. Because the GTP-binding capacity of LRRK2 is important for its kinase activity, we added guanine nucleotides (GTP and GDP) or their nonhydrolyzable

dx.doi.org/10.1021/bi400596m | *Biochemistry* 2013, 52, 6052−6062

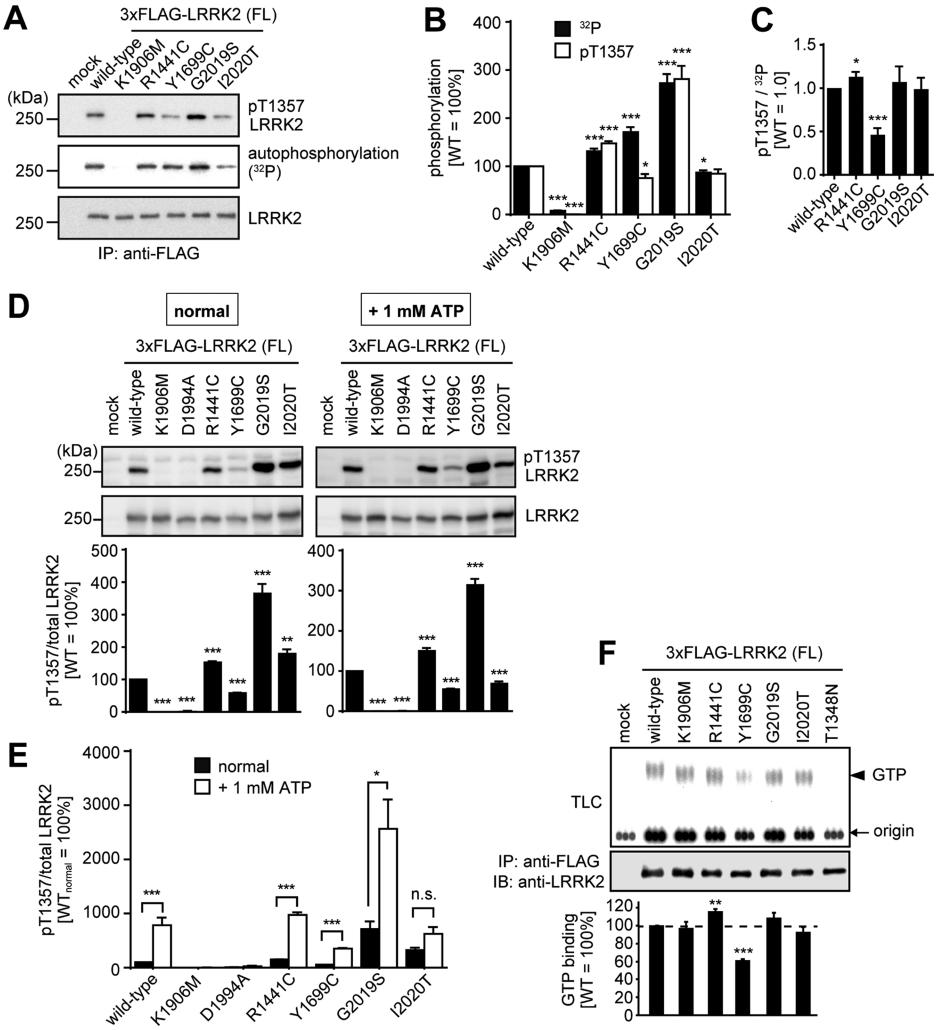

Figure 4. Effects of familial Parkinson mutations on the autophosphorylation at Thr1357 of LRRK2 in vitro as well as in cell lysates. (A) On-beads analysis by immunoblotting with the anti-pT1357 antibody (top panel; T1357 autophosphorylation) as well as by autoradiography (middle panel; total autophosphorylation). (B) Quantification of panel A. The levels of the T1357 autophosphorylation (white) and the total autophosphorylation (black) were quantified and normalized by the expression levels of LRRK2 determined by immunoblotting with the anti-LRRK2 antibody (bottom panel in A). The data are given as the percentage of those observed in WT LRRK2 (n = 3, mean ± standard error). *p < 0.05 and ***p < 0.001 (Student's t test; compared with WT). (C) Ratio of T1357 autophosphorylation that comprised the total autophosphorylation determined in panel B. *p < 0.05 and ***p < 0.001 (Student's t test; compared with WT). (D) HEK293 cell lysates (0.5 mg/mL) were incubated in the absence (left) or presence (right) of 1 mM ATP for 5 min and subjected to immunoblotting. The levels of the T1357 autophosphorylation (top panel) were quantified and normalized by the expression levels of LRRK2 determined by immunoblotting with the anti-LRRK2 antibody (MJFF2; bottom panel). The data are given as the percentage of those observed in WT LRRK2 (n = 3, mean ± standard error). **p < 0.01 and ***p < 0.001 (Student's t test; compared with WT). (E) Autophosphorylation at Thr1357 in the presence (white) or absence (black) of externally added ATP. The data are given as the percentage of those observed in WT LRRK2 under normal (ATP(−)) conditions (n = 3−5, mean ± standard error). *p < 0.05 and ***p < 0.001 (Student's t test; compared with normal condition). n.s., not significant. (F) In-cell GTP binding of LRRK2 harboring familial Parkinson mutations. HEK293 cells overexpressing FL-3×FLAG-LRRK2 were metabolically labeled with [^{32}P]-orthophosphate, and the bound GTP was analyzed by TLC. Radiolabeled GTP was visualized by autoradiography, and the radioactivity was quantified. The data are given as the percentage of those observed in WT LRRK2 (n = 3, mean ± standard error). **p < 0.01 and ***p < 0.001 (Student's t test; compared with WT).

analogs (guanosine 5′-*O*-[γ-thio]triphosphate (GTPγS) and guanylyl imidodiphosphate (GMP-PNP)) to cell lysates and examined their effects on the in-lysate autophosphorylation of LRRK2. The addition of 10 μM GTP to lysates of HEK293 cells overexpressing FL-LRRK2 showed no significant effect on the in-lysate autophosphorylation of FL-LRRK2 at Thr1357, whereas the addition of 10 μM GDP reduced the in-lysate autophosphorylation of FL-LRRK2 at Thr1357 to ∼60% of that of the nontreatment (Figure S2E). A similar reduction in the in-lysate autophosphorylation at Thr1357 was observed upon the addition of 10 μM GTPγS or 100 μM GMP-PNP (Figure S2E). These results suggested that inhibition of the GTP hydrolysis activity in cell lysates reduces the in-lysate autophosphorylation of LRRK2.

Effect of Familial Mutations on Autophosphorylation at Thr1357. We examined the effect of pathogenic mutations of LRRK2 on autophosphorylation at Thr1357 by the conventional on-beads assay. When we examined the total autophosphorylation of the six pathogenic mutants (i.e., R1441C/G/H, Y1699C, G2019S, and I2020T) by an in vitro assay using [γ-^{32}P]ATP, we observed a significant increase in the total autophosphorylation in R1441C, Y1699C, and G2019S LRRK2, whereas I2020T LRRK2 exhibited a rather decreased phosphorylation compared with that of WT LRRK2 (Figure 4A,B; black bar).

dx.doi.org/10.1021/bi400596m | *Biochemistry* 2013, 52, 6052−6062

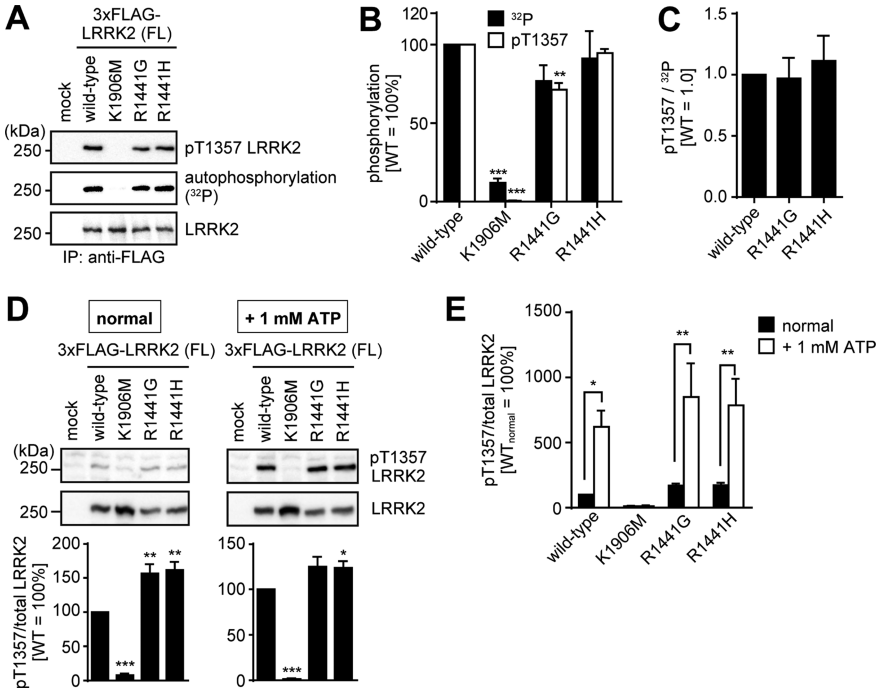

Figure 5. Effects of R1441G and R1441H mutations on the autophosphorylation at Thr1357 of LRRK2 in vitro as well as in cell lysates. (A) On-beads analysis by immunoblotting with the anti-pT1357 antibody (top panel; T1357 autophosphorylation) as well as by autoradiography (middle panel; total autophosphorylation). (B) Quantification of panel A. The levels of the T1357 autophosphorylation (white) and the total autophosphorylation (black) were quantified and normalized by the expression levels of LRRK2 determined by immunoblotting with the anti-LRRK2 antibody (MJFF2; bottom panel in A). The data are given as the percentage of those observed in WT LRRK2 (n = 3, mean ± standard error). $^{**}p < 0.01$ and $^{***}p < 0.001$ (Student's t test; compared with WT). (C) Ratio of T1357 autophosphorylation that comprised the total autophosphorylation determined in panel B. (D) HEK293 cell lysates (0.5 mg/mL) were incubated in the absence (left) or presence (right) of 1 mM ATP for 5 min and subjected to immunoblotting. The levels of the T1357 autophosphorylation (top panel) were quantified and normalized by the expression levels of LRRK2 determined by immunoblotting with the anti-LRRK2 antibody (MJFF2; bottom panel). The data are given as the percentage of those observed in WT LRRK2 (n = 3, mean ± standard error). $^{*}p < 0.05$, $^{**}p < 0.01$, and $^{***}p < 0.001$ (Student's t test; compared with WT). (E) Autophosphorylation at Thr1357 in the presence (white) or absence (black) of externally added ATP. The data are given as the percentage of those observed in WT LRRK2 under normal (ATP(−)) conditions (n = 3, mean ± standard error). $^{*}p < 0.05$ and $^{**}p < 0.01$ (Student's t test; compared with normal condition).

We observed no significant differences among WT, R1441G, and R1441H LRRK2 (Figure 5A,B; black bar). However, when we examined the autophosphorylation at Thr1357 by immunoblotting using the anti-pT1357 antibodies, the autophosphorylation at Thr1357 of Y1699C and I2020T LRRK2 was not increased, whereas those of R1441C and G2019S LRRK2 exhibited an increase compared with that of WT LRRK2 (Figure 4A,B; white bar). R1441G LRRK2 exhibited reduced autophosphorylation at Thr1357 compared with that of WT LRRK2, whereas R1441H LRRK2 showed comparable autophosphorylation at Thr1357 (Figure 5A,B; white bar). The ratio of autophosphorylation at Thr1357 that composes the total autophosphorylation (pT1357/total) was significantly decreased in Y1699C LRRK2 (Figure 4C), suggesting that autophosphorylation at Thr1357 is downregulated in Y1699C LRRK2. The pT1357/total ratio was slightly but significantly increased in R1441C LRRK2 (Figure 4C), suggesting that autophosphorylation at Thr1357 is upregulated in R1441C LRRK2. The pT1357/total ratio of R1441G and R1441H LRRK2 were comparable to that of WT LRRK2 (Figure 5C). We then examined the in-lysate autophosphorylation at Thr1357 of LRRK2 harboring familial mutations to investigate the effect of familial mutations on the kinase activity of LRRK2 in cell lysates. In cell lysates, R1441C, R1441G, R1441H, G2019S, and I2020T LRRK2 showed significantly increased autophosphorylation compared with WT LRRK2 (Figures 4D and 5D; left panel). R1441G and R1441H LRRK2 exhibited increased autophosphorylation at Thr1357 in cell lysates (Figure 5D), although they exhibited comparable or slightly decreased kinase activities in vitro (Figure 5A, 5B), suggesting that the kinase activities of these mutants are enhanced by other proteins existing in the cell lysates. Notably, I2020T LRRK2 showed rather decreased autophosphorylation in cell lysates compared with WT LRRK2 when 1 mM ATP was added to the lysate, whereas R1441C, R1441G, R1441H, and G2019S LRRK2 exhibited an increase in autophosphorylation compared with WT LRRK2, suggesting a difference in the binding affinity for ATP (Figures 4D and 5D; right panel). Y1699C LRRK2 exhibited a decrease in autophosphorylation regardless of the concentration of ATP (Figure 4D), which might be attributed to the alteration in the pT1357/total ratio (Figure 4C). A comparison between the levels of in-lysate autophosphorylation at Thr1357 in the absence and presence of additional ATP revealed that I2020T LRRK2 poorly responded to added ATP, whereas other mutations increased the in-lysate autophosphorylation in response to the addition of ATP (Figures 4E and 5E). Consistent with the alteration of the pT1357/total ratio, we found that R1441C and Y1699C mutations caused an increase and a decrease in GTP binding, respectively (Figure 4F), suggesting that the conformation of the ROC domain is altered by these mutations.

Effects of Familial Mutations on the Km for ATP. We developed a kinase assay system using a synthetic peptide consisting of the amino acid sequence flanking Thr1357 (T1357tide) amino-terminally conjugated with a biotin moiety. Phosphorylation of T1357tide by LRRK2 was detected by

dx.doi.org/10.1021/bi400596m | Biochemistry 2013, 52, 6052−6062

enzyme-linked immunosorbent assay (ELISA) with a monoclonal anti-pT1357 antibody. (Figure 6A–C). When we

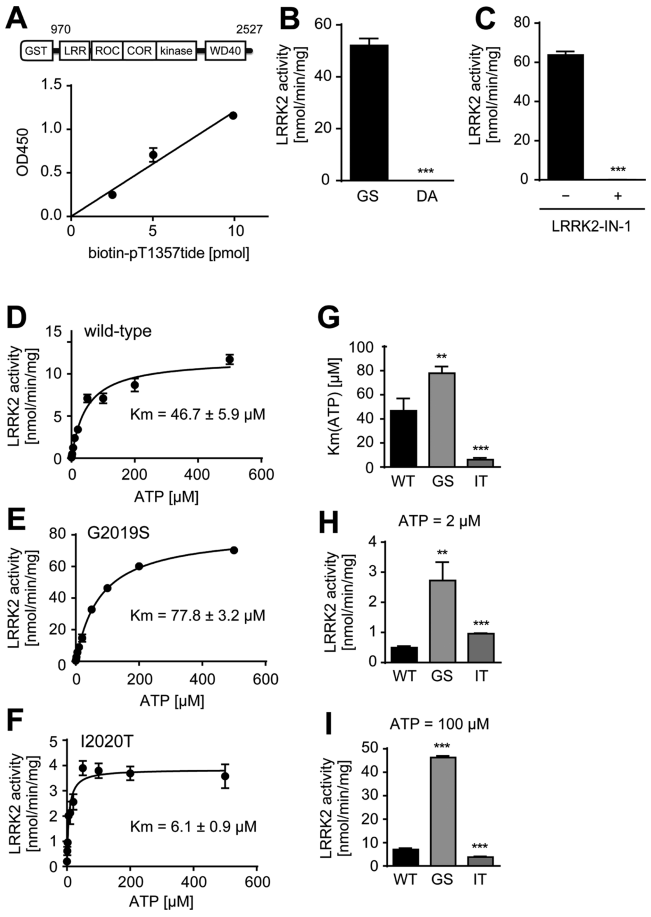

Figure 6. Determination of K_m(ATP) of LRRK2 harboring familial mutations. (A) Schematic representation of GST-ΔN-LRRK2 (970–2527 aa) and a standard curve of the in vitro assay system for LRRK2. The bpT1357tide was applied onto the streptavidin plate in duplicate. The phosphorylation of bT1357tide was detected by ELISA using the monoclonal anti-pT1357 antibody. OD, optical density. (B) bT1357tide was incubated with G2019S or D1994A GST-ΔN-LRRK2 (970–2527 aa) for 10 min at 30 °C, and the phosphorylation of the bT1357tide was examined by ELISA. ***$p < 0.001$ (Student's t test; compared with G2019S). (C) bT1357tide was incubated with G2019S GST-ΔN-LRRK2 (970–2527) for 15 min at 30 °C in the presence or absence of 3 μM LRRK2-IN-1, and the phosphorylation of bT1357tide was examined by ELISA. ***$p < 0.001$ (Student's t test; compared with LRRK2-IN-1(−)). (D, F) Michaelis–Menten plots for the determination of the apparent K_m(ATP) of wild-type (D), G2019S (E), and I2020T (F) GST-ΔN-LRRK2 (970–2527). (G) Calculated K_m(ATP) for LRRK2. **$p < 0.01$ and ***$p < 0.001$ (Student's t-test; compared with WT). (H, I) LRRK2 activity when the concentration of ATP was 2 (H) and 100 μM (I). The results are representative of three independent experiments performed in triplicate (mean ± standard deviation). **$p < 0.01$ and ***$p < 0.001$ (Student's t test; compared with WT).

quantitated the K_m for ATP (K_m(ATP)) of WT or familial Parkinson mutant LRRK2 using recombinant GST-ΔN-LRRK2 (970–2527 aa) by examining their kinase activity in the presence of various concentration of ATP, the K_m(ATP) values of WT, G2019S, and I2020T LRRK2 were 46.7 ± 5.9, 77.8 ± 3.2, and 6.1 ± 0.9 μM, respectively (Figure 6D,F). The significantly lower K_m(ATP) of I2020T LRRK2 compared to that of WT LRRK2 (Figure 6G) indicates that the kinase activity of I2020T LRRK2 in the presence of 2 μM ATP is significantly higher than that of WT LRRK2 (Figure 6H), whereas that of I2020T LRRK2 in the presence of 100 μM ATP is significantly lower than that of WT LRRK2 (Figure 6I). These results indicated that the kinase activity of I2020T LRRK2 reached the maximum in the presence of a lower concentration of ATP compared with WT LRRK2, which might explain its poor response to ATP in cell lysates (Figure 4E).

DISCUSSION

Elucidation of the effect of the familial mutations in LRRK2 on its functions or biochemical properties is crucial to the understanding of how these mutations cause neurodegeneration in PD. To investigate the involvement of the LRRK2 kinase activity in its neurotoxicity, we systematically characterized the autophosphorylation of LRRK2 by phosphopeptide mapping and found that LRRK2 is autophosphorylated at Thr1348, Thr1349, and Thr1357 in vitro and that the Y1699C mutation significantly reduces the autophosphorylation at Thr1357. We also established a unique in-lysate kinase assay, which enables the direct evaluation of the LRRK2 kinase activity in cell lysates. Using this assay, we found that I2020T LRRK2 exhibits an increased kinase activity compared to WT LRRK2 in the presence of a low concentration of ATP.

In this study, we characterized the autophosphorylation of LRRK2 by the phosphopeptide mapping method instead of mass spectrometry because the phosphopeptide mapping enables us to investigate the whole set of autophosphorylation in a single assay in a semiquantitative manner. We showed that most spots in the map of GST-ΔN-LRRK2 were also observed in that of GST-ROC (Figure 1C), suggesting that the majority of the autophosphorylation in ΔN-LRRK2 occurs in the ROC domain. This is consistent with the report by Gloeckner and colleagues who showed that the autophosphorylation of LRRK2 occurs mainly in the ROC domain.[25] By substitution of each Thr residue in the ROC domain with Ala, we identified Thr1348, Thr1349, and Thr1357 as the major autophosphorylation sites (Figures 1B,D and S1A). Although we and others have previously reported that LRRK2 is autophosphorylated at Thr1410, Thr1491, and Thr1503 in vitro,[24,26,27] autophosphorylation of these residues seems to be minor because Ala substitution of these residues caused little effect on the spot pattern of the phosphopeptide maps (Figure S1B). Spots that did not disappear by substitution of any threonines in the ROC domain might correspond to (i) autophosphorylation outside the ROC domain, (ii) autophosphorylation at serine residues in the ROC domain, or (iii) huge peptides corresponding to missed cleavage products by trypsin.

In the crystal structure of the ROC domain, Thr1349 is located within the P-loop, which is a conserved structure among GTP-binding proteins and is involved in the binding of the charged phosphate groups of nucleotides,[33] and the hydroxyl group of its side chain interacts with the α-phosphate of bound GDP.[34] Because Asp substitution of Thr1349 caused loss of guanine-nucleotide binding and Ala substitution was well-tolerated (Figure 2A), it is reasonable to speculate that autophosphorylation at Thr1349 has a negative impact on guanine-nucleotide binding. However, Thr1357 is located at a distance from the GTP-binding pocket outside the P-loop in the crystal structure, which is consistent with our result that substitution of Thr1357 caused little effect on guanine-nucleotide binding (Figure 2A). Although autophosphorylation at Thr1357 does not seem to play

dx.doi.org/10.1021/bi400596m | Biochemistry 2013, 52, 6052–6062

an essential role in the regulation of guanine-nucleotide binding, there still remains the possibility that autophosphorylation at Thr1357 modulates protein−protein interactions or the GTPase activity of LRRK2.

Interestingly, we found that LRRK2 undergoes autophosphorylation in cell lysates (Figures 3 and S2). The autophosphorylation at Thr1357 in cell lysates was linearly increased up to 5 min, reached the plateau after ∼1−2 h of incubation, and decreased after prolonged incubation (Figures 3A and S2D). Although the autophosphorylation at Thr1357 efficiently occurred in cell lysates because it took place even at 4 °C (Figure 3D), we could not detect the autophosphorylation at Thr1357 without in vitro phosphorylation (Figure 3A; input, Figure S1C). On the basis of these findings, we concluded that LRRK2 is not stably autophosphorylated at Thr1357 within cells. We speculate that, within cells, dephosphorylation activity by unknown phosphatases against phospho-Thr1357 of LRRK2 might surpass the autophosphorylation activity of LRRK2 at Thr1357. When the responsible phosphatases are diluted upon lysis, the autophosphorylation activity of LRRK2 might become predominant over dephosphorylation. Because prolonged incubation has been reported to downregulate the autophosphorylation activity of LRRK2 in vitro,[27] dephosphorylation would again become predominant over autophosphorylation after prolonged incubation (Figure S2D). The dephosphorylation activity against phospho-Thr1357 of LRRK2 should be higher in cell lysates with higher protein concentration, which might cause the less efficient autophosphorylation of LRRK2 under this condition (Figure 3C). Alternatively, it is possible that the sensitivity of our anti-pT1357 antibodies used in this study is not high enough for the detection of the in-cell autophosphorylation at Thr1357 of LRRK2. Nevertheless, considering that the existing kinase assays for LRRK2 require purified LRRK2, the present system has the advantage that we can examine LRRK2 activity without purification. Because the in-lysate autophosphorylation of endogenous LRRK2 is detectable (Figure 3B) and it occurs not only at Thr1357 but also at Thr1410 or Thr1491 (Figure S2C), in-lysate autophosphorylation would be a convenient tool to evaluate the kinase activity of LRRK2.

In an attempt to examine the effect of guanine nucleotides on the in-lysate autophosphorylation, we found that the addition of GDP, GTPγS, or GMP-PNP caused a significant reduction in the in-lysate autophosphorylation (Figure S2E). Because several reports have suggested that the addition of guanine nucleotides or their nonhydrolyzable analogs to purified LRRK2 has no effect on its kinase activity,[32,35] it is not likely that the added GDP, GTPγS, or GMP-PNP directly bound to FL-LRRK2 in cell lysates, thereby reducing its in-lysate autophosphorylation. We speculate that GDP, GTPγS, or GMP-PNP bind to guanine-nucleotide binding proteins in cell lysates other than LRRK2. Because the addition of both GDP and nonhydrolyzable analogs of GTP decreased the in-lysate autophosphorylation (Figure S2E), the GTP-hydrolysis activity of unknown proteins, but not GTP/GDP binding, would be important for the autophosphorylation of LRRK2 in cell lysates. The down-regulation of autophosphorylation of LRRK2 by the addition of GDP or nonhydrolyzable analogs into cell lysates is inconsistent with the previous reports showing increased autophosphorylation of LRRK2.[32,36] The precise reason for this inconsistency is unclear at this stage, but it might be due to the difference of the experimental system: in the previous reports, purified LRRK2 was used to examine the autophosphorylation activity after incubation in the presence of guanine nucleotides or their analogs in cell lysates, whereas the autophosphorylation of LRRK2 was directly examined in cell lysates in the presence of guanine nucleotides or their analogs in this study. Given that the in-lysate autophosphorylation of LRRK2 was modulated by other guanine-nucleotide binding proteins, further investigation into the in-lysate autophosphorylation of LRRK2 could uncover the mechanism of the upstream regulation of LRRK2 kinase activity by guanine-nucleotide binding proteins.

As shown in Figures 4 and 5, we carefully compared the total autophosphorylation of LRRK2 using [γ-^{32}P] ATP with the autophosphorylation at Thr1357 using a specific antibody against phosphorylated Thr1357 and found that R1441C and Y1699C mutations significantly alter the ratio of pT1357 in the total autophosphorylation (Figures 4A−C and 5A−C). Because it has been shown in a homologous protein (*Chlorobium tepidum* Roco protein) harboring a ROC−COR tandem domain that the residues corresponding to Arg1441 and Tyr1699 of LRRK2 are located at the ROC/COR interface,[37] it is possible that the conformation of the ROC domain was compromised by both mutations, leading to a significant alteration in the autophosphorylation at Thr1357. Because the R1441G and R1441H mutations caused no effect on the pT1357/total ratio (Figure 5C), Cys substitution, but not Gly nor His substitution, of Arg1441 might be critical to alter the conformation of the ROC domain. Notably, using the in-lysate autophosphorylation assay, I2020T LRRK2 exhibited a significant increase in autophosphorylation (Figure 4D; left panel). This result contradicted with the observation that I2020T LRRK2 failed to exhibit increased autophosphorylation in a conventional on-beads assay (Figure 4A,B). Interestingly, when we added 1 mM ATP to the lysate, autophosphorylation at Thr1357 of I2020T LRRK2 was not significantly changed, whereas those of the other mutants were increased (Figures 4E and 5E). One possible interpretation of these results would be that the kinase activity of I2020T LRRK2 already reaches the maximum at a low concentration of ATP and is not further upregulated by the addition of ATP. In support of this interpretation, Reichling and colleagues have examined the K_m for ATP (K_m(ATP)) of WT, G2019S and I2020T LRRK2 using LRRKtide as a substrate and concluded that the K_m(ATP) of I2020T LRRK2 is significantly lower than those of WT and G2019S LRRK2.[38] We confirmed this notion by an originally established kinase assay using the amino acid sequence flanking Thr1357 (T1357tide) as a substrate (Figure 6). Collectively, the observation that I2020T LRRK2 undergoes autophosphorylation more efficiently than WT LRRK2 in cell lysate is attributable to the difference in the K_m(ATP) between WT and I2020T LRRK2. Considering that I2020T mutation fails to upregulate the kinase activity in the presence of a high concentration of ATP, we speculate that I2020T LRRK2 does not exhibit higher activity compared with WT LRRK2 under physiological conditions (ATP concentration of 1−10 mM). Nevertheless, given that all familial Parkinson mutants except Y1699C, which was not analyzable because of the altered pT1357/total ratio, showed an increase in the in-lysate autophosphorylation under normal assay conditions (i.e., low ATP concentration), it is tempting to speculate that an abnormal reduction in the concentration of ATP caused by, for example, mitochondrial failure confers a relatively higher activity on LRRK2 harboring familial Parkinson mutations compared with WT, which may be toxic to neurons.

We systematically characterized the autophosphorylation of LRRK2 for the first time by phosphopeptide mapping and established a unique and useful method to examine the kinase

activity of LRRK2 using cell lysates. Further investigation into the effect of the pathogenic mutations in LRRK2 would provide clues for the elucidation of the molecular mechanism(s) of neurodegeneration caused by LRRK2.

■ ASSOCIATED CONTENT

Supporting Information

Sequences of the primers used for mutagenesis, 2D TLC analysis of LRRK2, and in-lysate autophosphorylation of LRRK2. This material is available free of charge via the Internet at http://pubs.acs.org.

■ AUTHOR INFORMATION

Corresponding Author

*Phone: 81-3-5841-3541; Fax: 81-3-5841-3613; E-mail: iwatsubo@m.u-tokyo.ac.jp.

Author Contributions

§These authors contributed equally to this work.

Funding

This work was supported by the Japan Society for the Promotion of Science (grant nos. 22790058 and 24790068 to G.I.), a Grant-in-Aid for Young Scientists (B) from the Ministry of Education, Culture, Sports, Science and Technology (grant no. 17025009 to T.I.), a Grant-in-Aid for Scientific Research on Priority Areas-Research on Pathomechanism of Brain Disorders, and Global Center of Excellence Program from the Japan Science and Technology Agency (Core Research for Evolutional Science and Technology (CREST) to T.I.), and Elan Pharmaceuticals (Innovation Program).

Notes

The authors declare no competing financial interest.

■ ACKNOWLEDGMENTS

We thank Drs. John Anderson, Zhao Ren, Dale Schenk, and other scientists at Elan Pharmaceuticals as well as current and former lab members for helpful discussions and technical assistance.

■ ABBREVIATIONS

LRRK2, leucine-rich repeat kinase 2; LRR, leucine-rich repeat; ROC, Ras of complex proteins; COR, carboxyl-terminal of ROC; WT, wild type; TLC, thin-layer chromatography; IB, immunoblotting

■ REFERENCES

(1) Fahn, S. (2003) Description of Parkinson's disease as a clinical syndrome. *Ann. N. Y. Acad. Sci. 991*, 1−14.

(2) Spillantini, M. G., Schmidt, M. L., Lee, V. M., Trojanowski, J. Q., Jakes, R., and Goedert, M. (1997) Alpha-synuclein in Lewy bodies. *Nature 388*, 839−840.

(3) Baba, M., Nakajo, S., Tu, P. H., Tomita, T., Nakaya, K., Lee, V. M., Trojanowski, J. Q., and Iwatsubo, T. (1998) Aggregation of alpha-synuclein in Lewy bodies of sporadic Parkinson's disease and dementia with Lewy bodies. *Am. J. Pathol. 152*, 879−884.

(4) Paisan-Ruiz, C., Jain, S., Evans, E. W., Gilks, W. P., Simon, J., van der Brug, M., Lopez de Munain, A., Aparicio, S., Gil, A. M., Khan, N., Johnson, J., Martinez, J. R., Nicholl, D., Carrera, I. M., Pena, A. S., de Silva, R., Lees, A., Marti-Masso, J. F., Perez-Tur, J., Wood, N. W., and Singleton, A. B. (2004) Cloning of the gene containing mutations that cause PARK8-linked Parkinson's disease. *Neuron 44*, 595−600.

(5) Zimprich, A., Biskup, S., Leitner, P., Lichtner, P., Farrer, M., Lincoln, S., Kachergus, J., Hulihan, M., Uitti, R. J., Calne, D. B., Stoessl, A. J., Pfeiffer, R. F., Patenge, N., Carbajal, I. C., Vieregge, P., Asmus, F., Muller-Myhsok, B., Dickson, D. W., Meitinger, T., Strom, T. M., Wszolek, Z. K., and Gasser, T. (2004) Mutations in LRRK2 cause autosomal-dominant parkinsonism with pleomorphic pathology. *Neuron 44*, 601−607.

(6) Haugarvoll, K., and Wszolek, Z. K. (2009) Clinical features of LRRK2 parkinsonism. *Parkinsonism Relat. Disord. 15*, S205−S208.

(7) Satake, W., Nakabayashi, Y., Mizuta, I., Hirota, Y., Ito, C., Kubo, M., Kawaguchi, T., Tsunoda, T., Watanabe, M., Takeda, A., Tomiyama, H., Nakashima, K., Hasegawa, K., Obata, F., Yoshikawa, T., Kawakami, H., Sakoda, S., Yamamoto, M., Hattori, N., Murata, M., Nakamura, Y., and Toda, T. (2009) Genome-wide association study identifies common variants at four loci as genetic risk factors for Parkinson's disease. *Nat. Genet. 41*, 1303−1307.

(8) Simon-Sanchez, J., Schulte, C., Bras, J. M., Sharma, M., Gibbs, J. R., Berg, D., Paisan-Ruiz, C., Lichtner, P., Scholz, S. W., Hernandez, D. G., Kruger, R., Federoff, M., Klein, C., Goate, A., Perlmutter, J., Bonin, M., Nalls, M. A., Illig, T., Gieger, C., Houlden, H., Steffens, M., Okun, M. S., Racette, B. A., Cookson, M. R., Foote, K. D., Fernandez, H. H., Traynor, B. J., Schreiber, S., Arepalli, S., Zonozi, R., Gwinn, K., van der Brug, M., Lopez, G., Chanock, S. J., Schatzkin, A., Park, Y., Hollenbeck, A., Gao, J., Huang, X., Wood, N. W., Lorenz, D., Deuschl, G., Chen, H., Riess, O., Hardy, J. A., Singleton, A. B., and Gasser, T. (2009) Genome-wide association study reveals genetic risk underlying Parkinson's disease. *Nat. Genet. 41*, 1308−1312.

(9) Cookson, M. R. (2010) The role of leucine-rich repeat kinase 2 (LRRK2) in Parkinson's disease. *Nat. Rev. Neurosci. 11*, 791−797.

(10) Smith, W. W., Pei, Z., Jiang, H., Dawson, V. L., Dawson, T. M., and Ross, C. A. (2006) Kinase activity of mutant LRRK2 mediates neuronal toxicity. *Nat. Neurosci. 9*, 1231−1233.

(11) Ito, G., Okai, T., Fujino, G., Takeda, K., Ichijo, H., Katada, T., and Iwatsubo, T. (2007) GTP binding is essential to the protein kinase activity of LRRK2, a causative gene product for familial Parkinson's disease. *Biochemistry 46*, 1380−1388.

(12) West, A. B., Moore, D. J., Choi, C., Andrabi, S. A., Li, X., Dikeman, D., Biskup, S., Zhang, Z., Lim, K. L., Dawson, V. L., and Dawson, T. M. (2007) Parkinson's disease-associated mutations in LRRK2 link enhanced GTP-binding and kinase activities to neuronal toxicity. *Hum. Mol. Genet. 16*, 223−232.

(13) Healy, D. G., Falchi, M., O'Sullivan, S. S., Bonifati, V., Durr, A., Bressman, S., Brice, A., Aasly, J., Zabetian, C. P., Goldwurm, S., Ferreira, J. J., Tolosa, E., Kay, D. M., Klein, C., Williams, D. R., Marras, C., Lang, A. E., Wszolek, Z. K., Berciano, J., Schapira, A. H., Lynch, T., Bhatia, K. P., Gasser, T., Lees, A. J., and Wood, N. W. (2008) Phenotype, genotype, and worldwide genetic penetrance of LRRK2-associated Parkinson's disease: a case-control study. *Lancet Neurol. 7*, 583−590.

(14) Ozelius, L. J., Senthil, G., Saunders-Pullman, R., Ohmann, E., Deligtisch, A., Tagliati, M., Hunt, A. L., Klein, C., Henick, B., Hailpern, S. M., Lipton, R. B., Soto-Valencia, J., Risch, N., and Bressman, S. B. (2006) LRRK2 G2019S as a cause of Parkinson's disease in Ashkenazi Jews. *N. Engl. J. Med. 354*, 424−425.

(15) West, A. B., Moore, D. J., Biskup, S., Bugayenko, A., Smith, W. W., Ross, C. A., Dawson, V. L., and Dawson, T. M. (2005) Parkinson's disease-associated mutations in leucine-rich repeat kinase 2 augment kinase activity. *Proc. Natl. Acad. Sci. U.S.A. 102*, 16842−16847.

(16) Gloeckner, C. J., Kinkl, N., Schumacher, A., Braun, R. J., O'Neill, E., Meitinger, T., Kolch, W., Prokisch, H., and Ueffing, M. (2006) The Parkinson disease causing LRRK2 mutation I2020T is associated with increased kinase activity. *Hum. Mol. Genet. 15*, 223−232.

(17) Jaleel, M., Nichols, R. J., Deak, M., Campbell, D. G., Gillardon, F., Knebel, A., and Alessi, D. R. (2007) LRRK2 phosphorylates moesin at threonine-558: characterization of how Parkinson's disease mutants affect kinase activity. *Biochem. J. 405*, 307−317.

(18) Nichols, R. J., Dzamko, N., Hutti, J. E., Cantley, L. C., Deak, M., Moran, J., Bamborough, P., Reith, A. D., and Alessi, D. R. (2009) Substrate specificity and inhibitors of LRRK2, a protein kinase mutated in Parkinson's disease. *Biochem. J. 424*, 47−60.

(19) Li, X., Tan, Y. C., Poulose, S., Olanow, C. W., Huang, X. Y., and Yue, Z. (2007) Leucine-rich repeat kinase 2 (LRRK2)/PARK8

possesses GTPase activity that is altered in familial Parkinson's disease R1441C/G mutants. *J. Neurochem. 103*, 238−247.
(20) Kawakami, F., Yabata, T., Ohta, E., Maekawa, T., Shimada, N., Suzuki, M., Maruyama, H., Ichikawa, T., and Obata, F. (2012) LRRK2 phosphorylates tubulin-associated tau but not the free molecule: LRRK2-mediated regulation of the tau-tubulin association and neurite outgrowth. *PLoS One 7*, e30834-1−e30834-9.
(21) Matta, S., Van Kolen, K., da Cunha, R., van den Bogaart, G., Mandemakers, W., Miskiewicz, K., De Bock, P. J., Morais, V. A., Vilain, S., Haddad, D., Delbroek, L., Swerts, J., Chavez-Gutierrez, L., Esposito, G., Daneels, G., Karran, E., Holt, M., Gevaert, K., Moechars, D. W., De Strooper, B., and Verstreken, P. (2012) LRRK2 controls an EndoA phosphorylation cycle in synaptic endocytosis. *Neuron 75*, 1008−1021.
(22) Sheng, Z., Zhang, S., Bustos, D., Kleinheinz, T., Le Pichon, C. E., Dominguez, S. L., Solanoy, H. O., Drummond, J., Zhang, X., Ding, X., Cai, F., Song, Q., Li, X., Yue, Z., van der Brug, M. P., Burdick, D. J., Gunzner-Toste, J., Chen, H., Liu, X., Estrada, A. A., Sweeney, Z. K., Scearce-Levie, K., Moffat, J. G., Kirkpatrick, D. S., and Zhu, H. (2012) Ser1292 autophosphorylation is an indicator of LRRK2 kinase activity and contributes to the cellular effects of PD mutations. *Sci. Transl. Med. 4*, 164ra161.
(23) Greggio, E., Taymans, J. M., Zhen, E. Y., Ryder, J., Vancraenenbroeck, R., Beilina, A., Sun, P., Deng, J., Jaffe, H., Baekelandt, V., Merchant, K., and Cookson, M. R. (2009) The Parkinson's disease kinase LRRK2 autophosphorylates its GTPase domain at multiple sites. *Biochem. Biophys. Res. Commun. 389*, 449−454.
(24) Kamikawaji, S., Ito, G., and Iwatsubo, T. (2009) Identification of the autophosphorylation sites of LRRK2. *Biochemistry 48*, 10963−10975.
(25) Gloeckner, C. J., Boldt, K., von Zweydorf, F., Helm, S., Wiesent, L., Sarioglu, H., and Ueffing, M. (2010) Phosphopeptide analysis reveals two discrete clusters of phosphorylation in the N-terminus and the Roc domain of the Parkinson-disease associated protein kinase LRRK2. *J. Proteome Res. 9*, 1738−1745.
(26) Pungaliya, P. P., Bai, Y., Lipinski, K., Anand, V. S., Sen, S., Brown, E. L., Bates, B., Reinhart, P. H., West, A. B., Hirst, W. D., and Braithwaite, S. P. (2010) Identification and characterization of a leucine-rich repeat kinase 2 (LRRK2) consensus phosphorylation motif. *PLoS One 5*, e13672-1−e13672-13.
(27) Webber, P. J., Smith, A. D., Sen, S., Renfrow, M. B., Mobley, J. A., and West, A. B. (2011) Autophosphorylation in the leucine-rich repeat kinase 2 (LRRK2) GTPase domain modifies kinase and GTP-binding activities. *J. Mol. Biol. 412*, 94−110.
(28) Hashimoto, T., Wakabayashi, T., Watanabe, A., Kowa, H., Hosoda, R., Nakamura, A., Kanazawa, I., Arai, T., Takio, K., Mann, D. M. A., and Iwatsubo, T. (2002) CLAC: a novel Alzheimer amyloid plaque component derived from a transmembrane precursor, CLAC-P/collagen type XXV. *EMBO J. 21*, 1524−34.
(29) Ito, G., and Iwatsubo, T. (2012) Re-examination of the dimerization state of leucine-rich repeat kinase 2: predominance of the monomeric form. *Biochem. J. 441*, 987−994.
(30) Boyle, W. J., van der Geer, P., and Hunter, T. (1991) Phosphopeptide mapping and phosphoamino acid analysis by two-dimensional. *Methods Enzymol. 201*, 110−49.
(31) Nichols, R. J., Dzamko, N., Morrice, N. A., Campbell, D. G., Deak, M., Ordureau, A., Macartney, T., Tong, Y., Shen, J., Prescott, A. R., and Alessi, D. R. (2010) 14-3-3 binding to LRRK2 is disrupted by multiple Parkinson's disease-associated mutations and regulates cytoplasmic localization. *Biochem. J. 430*, 393−404.
(32) Taymans, J.-M., Vancraenenbroeck, R., Ollikainen, P., Beilina, A., Lobbestael, E., De Maeyer, M., Baekelandt, V., and Cookson, M. R. (2011) LRRK2 kinase activity is dependent on LRRK2 GTP binding capacity but independent of LRRK2 GTP binding. *PLoS One 6*, e23207-1−e23207-11.
(33) Taymans, J.-M. (2012) The GTPase function of LRRK2. *Biochem. Soc. Trans. 40*, 1063−1069.
(34) Deng, J., Lewis, P. A., Greggio, E., Sluch, E., Beilina, A., and Cookson, M. R. (2008) Structure of the ROC domain from the Parkinson's disease-associated leucine-rich repeat kinase 2 reveals a dimeric GTPase. *Proc. Natl. Acad. Sci. U.S.A. 105*, 1499−1504.
(35) Liu, M., Dobson, B., Glicksman, M. A., Yue, Z., and Stein, R. L. (2010) Kinetic mechanistic studies of wild-type leucine-rich repeat kinase 2: characterization of the kinase and GTPase activities. *Biochemistry 49*, 2008−2017.
(36) Biosa, A., Trancikova, A., Civiero, L., Glauser, L., Bubacco, L., Greggio, E., and Moore, D. J. (2013) GTPase activity regulates kinase activity and cellular phenotypes of Parkinson's disease-associated LRRK2. *Hum. Mol. Genet. 22*, 1140−1156.
(37) Gotthardt, K., Weyand, M., Kortholt, A., Van Haastert, P. J., and Wittinghofer, A. (2008) Structure of the Roc-COR domain tandem of C. tepidum, a prokaryotic homologue of the human LRRK2 Parkinson kinase. *EMBO J. 27*, 2239−2249.
(38) Reichling, L. J., and Riddle, S. M. (2009) Leucine-rich repeat kinase 2 mutants I2020T and G2019S exhibit altered kinase inhibitor sensitivity. *Biochem. Biophys. Res. Commun. 384*, 255−258.